Published in final edited form as:
Nano Lett. 2010 June 9; 10(6): 2168–2172. doi:10.1021/nl100890d.

Ultra-High Sensitivity Carbon Nanotube Agents for Photoacoustic Molecular Imaging in Living Mice

Adam de la Zerda[1,2,†], **Zhuang Liu**[3,4,†], **Sunil Bodapati**[1], **Robert Teed**[1], **Srikant Vaithilingam**[2], **Butrus T. Khuri-Yakub**[2], **Xiaoyuan Chen**[1,5], **Hongjie Dai**[3,*], and **Sanjiv Sam Gambhir**[1,6,*]

[1]Molecular Imaging Program at Stanford, Department of Radiology and Bio-X Program, Stanford University, Palo Alto, CA 94305, USA

[2]Department of Electrical Engineering Stanford University, Palo Alto, CA 94305, USA

[3]Department of Chemistry, Stanford University, Palo Alto, CA 94305, USA

[4]Functional Nano & Soft Materials Laboratory (FUNSOM), Soochow University, Suzhou, Jiangsu, 215123, China

[5]Laboratory for Molecular Imaging and Nanomedicine, National Institute of Biomedical Imaging and Bioengineering (NIBIB), National Institutes of Health (NIH), Bethesda, MD 20892, USA

[6]Department of Bioengineering, Stanford University, Palo Alto, CA 94305, USA

Abstract

Photoacoustic imaging is an emerging modality that overcomes to a great extent the resolution and depth limitations of optical imaging while maintaining relatively high-contrast. However, since many diseases will not manifest an endogenous photoacoustic contrast, it is essential to develop exogenous photoacoustic contrast agents that can target diseased tissue(s). Here we present a novel photoacoustic contrast agent, Indocyanine Green dye-enhanced single walled carbon nanotube (SWNT-ICG). We conjugated this contrast agent with cyclic Arg-Gly-Asp (RGD) peptides to molecularly target the $\alpha_v\beta_3$ integrins, which are associated with tumor angiogenesis. Intravenous administration of this tumor-targeted contrast agent to tumor-bearing mice showed significantly higher photoacoustic signal in the tumor than in mice injected with the untargeted contrast agent. The new contrast agent gave a markedly 300-times higher photoacoustic contrast in living tissues than previously reported SWNTs, leading to sub-nanomolar sensitivities. Finally, we show that the new contrast agent can detect ~20-times fewer cancer cells than previously reported SWNTs.

Photoacoustic imaging is an emerging modality based on the photoacoustic effect where light is converted into ultrasound waves that are detected outside the subject of interest[1]. Photoacoustic imaging has been used in numerous applications where intrinsic contrast is available such as visualizing blood vessels structure[2], thermal burns[3] and melanoma[4]. However, most diseases will not show photoacoustic contrast, thereby requiring the use of an exogenous contrast agent which will target the diseased tissue. The main challenge in designing such contrast agent remains creating an agent that produces sufficient photoacoustic signal in order to be detected in low concentration, while being able to target the diseased tissue(s). In

*sgambhir@stanford.edu; hdai1@stanford.edu.
†These authors contributed equally to this work

Supporting Information
Description of particles synthesis, photoacoustic imaging instrument, experimental procedures, statistical methods, and in-vitro characterization of the particles including serum-stability, photobleaching and cell-uptake study.

this work, we developed a new contrast agent which targets cancer-specific receptor in tumor-bearing mice while producing unprecedented sensitivity.

We have recently reported on the conjugation of cyclic Arg-Gly-Asp (RGD) peptides to pegylated single walled carbon nanotubes[5] (SWNT-RGD) and their use as photoacoustic imaging agents[6] to image $\alpha_v\beta_3$ integrins, which are over-expressed in tumor vasculature. The minimal detectable concentration of SWNT-RGD in living mice was previously calculated to be ~50 nM. In this work, we enhanced the photoacoustic signal of the SWNT-RGD, by attaching Indocyanine Green (ICG) dye to the surface of the nanotubes through pi-pi stacking interactions[7] (see **Supplementary Information** for more details). The ultra-high surface area of the nanotubes allows for highly efficient loading of aromatic molecules such as ICG on the nanotube surface creating a new kind of photoacoustic agent, SWNT-ICG-RGD (Fig. 1a). Control untargeted particles were conjugated to a mutated non-targeted peptide, RAD that does not bind to $\alpha_v\beta_3$ integrins.

The optical absorbance spectrum of the new SWNT-ICG nanoparticle reveals that at its peak absorbance, at 780 nm, the SWNT-ICG particles exhibited a 20-fold higher absorbance as compared with plain SWNTs (Fig. 1b). Importantly, SWNT-ICG-RGD had very similar optical spectrum as SWNT-ICG-RAD. We constructed a non-absorbing and non-scattering agarose phantom with inclusions of SWNT-ICG-RGD at increasing concentrations from 0.5 nM to 121.5 nM in multiples of 3 (n = 3 inclusions of each concentration). The photoacoustic signal produced by the SWNT-ICG-RGD particles correlated highly with the nanoparticle concentration (R^2=0.983) (Fig. 1c).

We further validated that the new particles are stable in serum (**see Supplementary Information** and Fig. S1). The particle's photobleaching (i.e., loss of optical absorption due to continuous light exposure of the dye component of the nanoparticle) was characterized and found to be relatively small, only 30% reduction in optical absorption after 60 min of laser irradiation at normal power density of 8 mJ/cm^2 (**see Supplementary Information** and Fig. S2). Finally, cell uptake studies showed specific binding of SWNT-ICG-RGD to U87MG cells compared with the control particles SWNT-ICG-RAD (**see Supplementary Information** and Fig. S3).

We then tested the particle's sensitivity in living subjects by subcutaneously injecting the lower back of mice (n = 3) with 30 μl of SWNT-ICG-RAD mixed with matrigel at increasing concentrations of 820 pM to 200 nM in multiples of 3. Matrigel alone produced no significant photoacoustic signal (data not shown). All animal experiments were performed in compliance with the Guidelines for the Care and Use of Research Animals established by the Stanford University Animal Studies Committee. Upon injection, the matrigel solidified, fixing the SWNT-ICG-RAD in place and three-dimensional (3D) ultrasound and photoacoustic images of the inclusions were acquired (Fig. 2a). While the ultrasound image visualized the mouse anatomy (e.g., skin and inclusion edges), the photoacoustic image revealed the SWNT-ICG-RAD contrast in the mouse. The photoacoustic signal from each inclusion was quantified using a three dimensional region of interest (ROI) drawn over the inclusion volume. We observed a linear correlation (R^2 = 0.97) between the SWNT-ICG-RAD concentration and the corresponding photoacoustic signal (Fig. 2b). Tissue background signal was calculated as the average photoacoustic signal in areas where no contrast agent was injected. Extrapolation of the signal-concentration graph reveals that 170 pM of SWNT-ICG-RAD gives the equivalent photoacoustic signal as the tissue background (i.e., signal to background ratio = 1). This value represents over 300-times improvement in sensitivity compared to plain SWNTs.

Finally, we tested the nanoparticles targeting ability in living mice. Mice bearing U87MG tumor xenografts (150 mm^3 in size) were injected through the tail vein (IV) with 200 μl of

either SWNT-ICG-RGD (targeted) or SWNT-ICG-RAD (untargeted control) particles (n = 4 mice per group) at a concentration of 1.2 μM. We acquired 3D photoacoustic and ultrasound images of the entire tumor area before and up to 4 hours after the injection. Mice injected with SWNT-ICG-RGD showed significantly higher photoacoustic signal in the tumor compared with the control group injected with SWNT-ICG-RAD (Fig. 3a). The ultrasound images were used for visualizing the boundaries of the tumor as well as to validate that no significant movement (beyond 100 μm) had occurred throughout the experiment. While the tumor's photoacoustic signal before the injection is primarily due to the tumor's blood content, the photoacoustic signal post-injection is due to both the blood and the SWNT-ICG particles. To subtract out the background blood signal, a subtraction image calculated as the 2 hour post-injection minus the pre-injection image was calculated (Fig. 3a). Measurement of the photoacoustic signal from a 3D ROI around the tumor (Fig. 3b) showed that the photoacoustic signal in the tumor was significantly higher in mice injected with SWNT-ICG-RGD as compared with the control particles SWNT-ICG-RAD ($p < 0.001$). For example, at 2 hours post-injection, mice injected with SWNT-ICG-RGD showed over 100% higher photoacoustic signal in the tumor than mice injected with the control SWNT-ICG-RAD.

To compare the performance of plain SWNT-RGD to the dye-enhanced SWNT-ICG-RGD, we incubated U87MG cells, which express the target $\alpha_v\beta_3$ on their surface, with either particle solution for 2 hours. After incubation, the cells were washed 3 times with cold saline to remove unbound particles and placed in a clear agarose phantom at increasing concentrations from 25×10^3 to 6×10^6 cells per well (n = 3 samples per group) and imaged with the photoacoustic system (Fig. 4a). Quantitative analysis of the photoacoustic signal from the phantom revealed that cells exposed to SWNT-ICG-RGD were detected at 20-times lower concentration than cells exposed to plain SWNT-RGD ($p < 0.0001$) (Fig. 4a-b). These observations are consistent with the optical absorbance of SWNT-ICG-RGD being ~20 times higher than plain SWNT-RGD.

We have synthesized, characterized and demonstrated the application of dye-enhanced SWNTs as ultra-high sensitivity photoacoustic imaging agents. A concentration of 170 pM was estimated to produce an equivalent photoacoustic signal as tissue background signal, representing 300-times improvement in sensitivity as compared with plain SWNTs in living mice. This improvement is likely due to both the higher optical absorption of the particles as well as the fact that the new particle's absorption peak is at 780nm where the background tissue photoacoustic signal is greatly reduced. Intravenous injection of RGD-targeted SWNT-ICG particles to tumor-bearing mice led to significantly greater accumulation of the particles in the tumor compared to non-targeted control particles. This *in-vivo* targeting study results are likely negatively influenced by the effect of photo-bleaching, where continued laser light exposure of the tumor caused reduction in the optical absorption (and photoacoustic signal) of the particles that were bound to the tumor. This primarily affects the targeted group, SWNT-ICG-RGD, and to a much lesser extent the untargeted group, SWNT-ICG-RAD, which continued to circulate through the animal's blood stream unexposed to laser irradiation. Therefore, it is likely that the difference between these two groups is even greater in reality than reflected in the results. Finally, we demonstrated the ability to detect 20-times fewer cancer cells when using SWNT-ICG-RGD as the imaging agent, as compared with plain SWNT-RGD. These results agree with the fact that SWNT-ICG has ~20 times greater optical absorbance compared to plain SWNT. Applications of the enhanced particles may therefore be exploited to lead to the earlier detection of cancer by providing the ability to detect smaller tumors.

Most of the work done on photoacoustic contrast agents has been focused on gold nanoparticles[8-10] as well as other kinds of nanoparticles[11, 12]. However, the main challenge that has yet been solved is the delivery of such agents to the tumor in sufficient amounts to create detectable and specific signal. This is likely due to the particles' large size that leads to

rapid clearance by the reticuloendothelial system (RES) upon intravenous injection, preventing the particles from accumulating at the tumor site. In contrast, the SWNTs used here are 1-2 nm in diameter and 50-300 nm in length. Since the dye we used was attached to the surface of the SWNTs, under the PEG, it is expected that the total particle size was not significantly changed, thereby allowing the particles to keep a favorable bio-distribution as previously reported[5]. Hence, the dye-enhanced SWNTs presented in this work offer unprecedented photoacoustic signal strengths while maintaining relatively small size allowing them to target tumors upon intravenous injection. We have also previously published pilot toxicology studies of the SWNTs with encouraging results in mouse models[13] as well as observed they are able to be excreted via the biliary pathway[14].

The reason for loading a SWNT with many small ICG dye molecules is the high efficiency of optical absorption of ICG dye compared to its weight. According to the parameter of optical absorption divided by weight, ICG is 7-times more efficient than SWNTs and ~8500-times more efficient than commercial gold nanorods with a peak absorption at 780 nm.

The dye-enhanced SWNT photoacoustic contrast agents reported here have the capability to bind to molecular targets in living animals while maintaining a very high photoacoustic signal. No other imaging modality or imaging agent can achieve sub-nM sensitivity at large depths of penetration and sub-millimeter spatial resolution as can be achieved with photoacoustic imaging of dye-enhanced SWNTs.

Supplementary Material

Refer to Web version on PubMed Central for supplementary material.

Acknowledgments

We would like to acknowledge funding from the National Institute of Health (NIH) grants NCI CCNE U54 CA119367 (SSG), NCI ICMIC P50 CA114747 (SSG), and the Canary Foundation for supporting this work. A. de la Zerda is partially funded from the Bio-X Graduate Student Fellowship and the DoD Breast Cancer Research Program – Pre-doctoral Traineeship Award. The authors would also like to thank J. Rosenberg for the statistical analysis and Omer Oralkan and Te-Jen Ma for useful discussions.

References

1. Xu MH, Wang LHV. Rev. Sci. Instrum 2006;77(4):041101–043100.
2. Maslov K, Zhang HF, Hu S, Wang LV. Opt Lett 2008;33(9):929–31. [PubMed: 18451942]
3. Zhang HF, Maslov K, Stoica G, Wang LV. J Biomed Opt 2006;11(5):054033. [PubMed: 17092182]
4. Zhang HF, Maslov K, Stoica G, Wang LV. Nat Biotechnol 2006;24(7):848–51. [PubMed: 16823374]
5. Liu Z, Cai W, He L, Nakayama N, Chen K, Sun X, Chen X, Dai H. Nat Nanotechnol 2007;2(1):47–52. [PubMed: 18654207]
6. de la Zerda A, Zavaleta C, Keren S, Vaithilingam S, Bodapati S, Liu Z, Levi J, Smith BR, Ma TJ, Oralkan O, Cheng Z, Chen X, Dai H, Khuri-Yakub BT, Gambhir SS. Nat Nanotechnol 2008;3(9):557–62. [PubMed: 18772918]
7. Liu Z, Sun X, Nakayama-Ratchford N, Dai H. ACS Nano 2007;1(1):50–56. [PubMed: 19203129]
8. Kim JW, Galanzha EI, Shashkov EV, Moon HM, Zharov VP. Nat Nanotechnol 2009;4(10):688–94. [PubMed: 19809462]
9. Eghtedari M, Oraevsky A, Copland JA, Kotov NA, Conjusteau A, Motamedi M. Nano Letters 2007;7(7):1914–8. [PubMed: 17570730]
10. Yang X, Skrabalak SE, Li ZY, Xia Y, Wang LV. Nano Lett 2007;7(12):3798–802. [PubMed: 18020475]
11. Kim G, Huang SW, Day KC, O'Donnell M, Agayan RR, Day MA, Kopelman R, Ashkenazi S. J Biomed Opt 2007;12(4):044020. [PubMed: 17867824]

12. Zhang Q, Iwakuma N, Sharma P, Moudgil BM, Wu C, McNeill J, Jiang H, Grobmyer SR. Nanotechnology 2009;20(39):395102. [PubMed: 19726840]

13. Schipper ML, Nakayama-Ratchford N, Davis CR, Kam NWS, Chu P, Liu Z, Sun X, Dai H, Gambhir SS. Nat Nano 2008;3(4):216–221.

14. Liu Z, Davis C, Cai W, He L, Chen X, Dai H. Proc Natl Acad Sci U S A 2008;105(5):1410–5. [PubMed: 18230737]

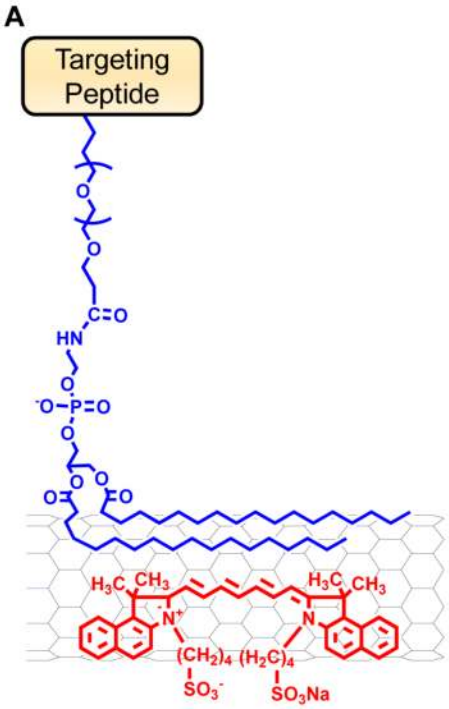

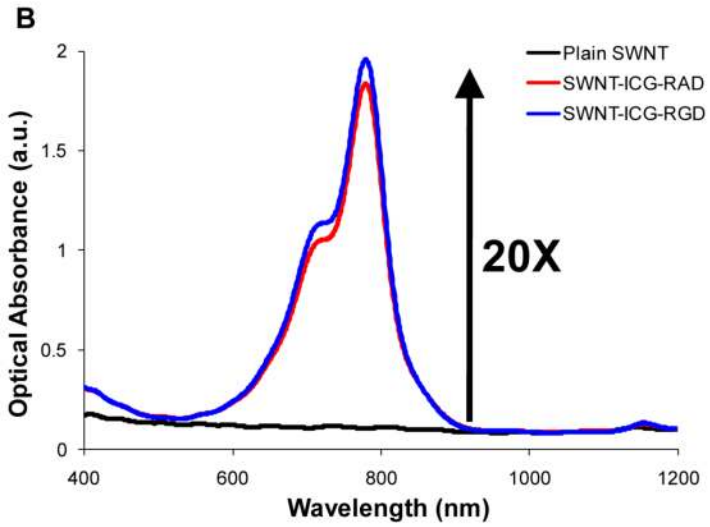

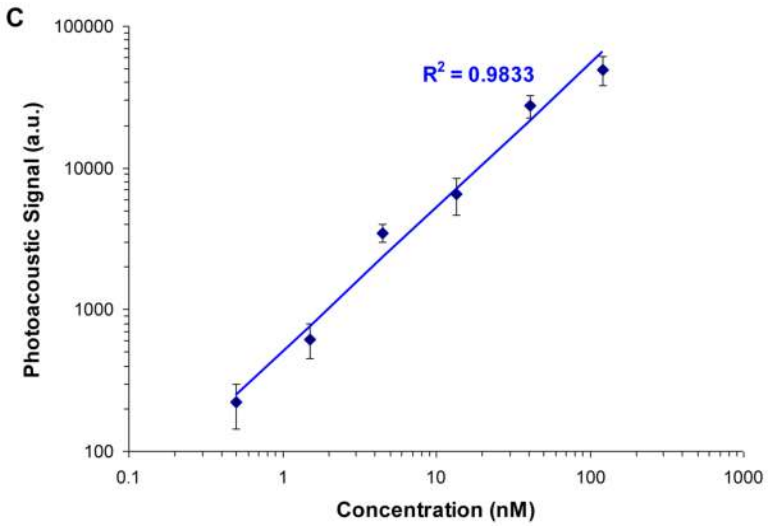

Figure 1. Characterization of the ICG dye-enhanced SWNT

(A) Illustration of a SWNT-ICG particle. ICG molecules (red) are attached to the SWNT surface through non-covalent pi-pi stacking bonds. Polyethylene glycol-5000 (blue) is conjugated to a targeting peptide in one end and to the SWNT surface on the other end through phospholipids. **(B)** Optical spectra of plain SWNT (black), SWNT-ICG-RGD (blue) and SWNT-ICG-RAD (red). ICG dye-enhanced SWNTs particles showed 20-times higher optical absorption than plain SWNT at the peak absorption wavelength, 780 nm. The similarity of SWNT-ICG-RAD and SWNT-ICG-RGD spectra suggests that the peptide conjugation does not notably perturb the photoacoustic signal. **(C)** The photoacoustic signal produced by SWNT-ICG was observed to be linearly dependent on the concentration ($R^2 = 0.9833$).

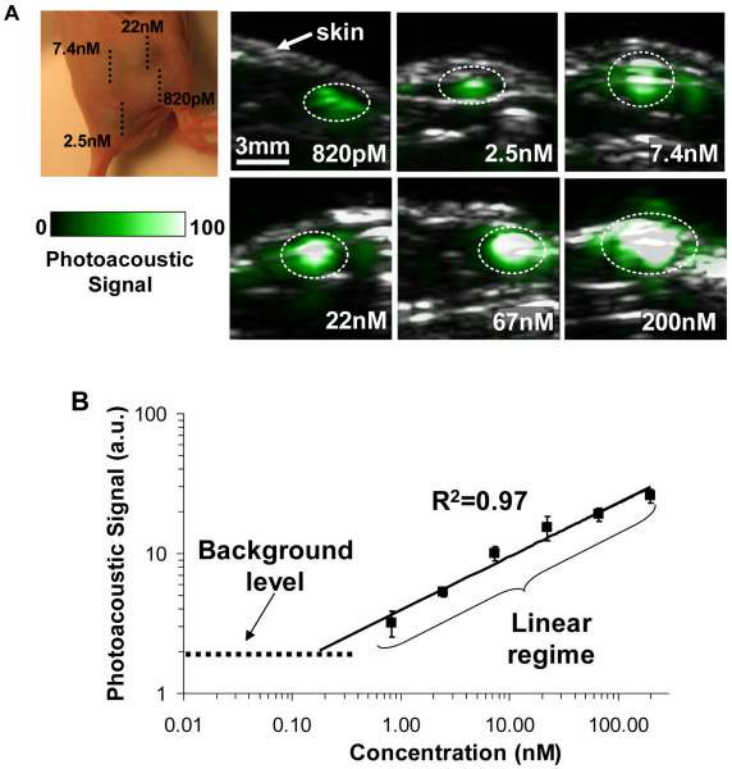

Figure 2. Photoacoustic detection of SWNT-ICG in living mice

(A) Mice were injected subcutaneously with SWNT-ICG at concentrations of 0.82-200 nM. The images represent ultrasound (gray) and photoacoustic (green) vertical slices through the subcutaneous injections (dotted black line). The skin is visualized in the ultrasound images, while the photoacoustic images show the SWNT-ICG distribution. The white dotted lines on the images illustrate the approximate edges of each inclusion. **(B)** The photoacoustic signal from each inclusion was calculated using 3D regions of interest and the 'background' represents the endogenous signal measured from tissues. The error bars represent standard error (n = 3 mice). Linear regression (R^2 = 0.97) of the photoacoustic signal curve estimates that a concentration of 170 pM of SWNT-ICG will give the equivalent background signal of tissues.

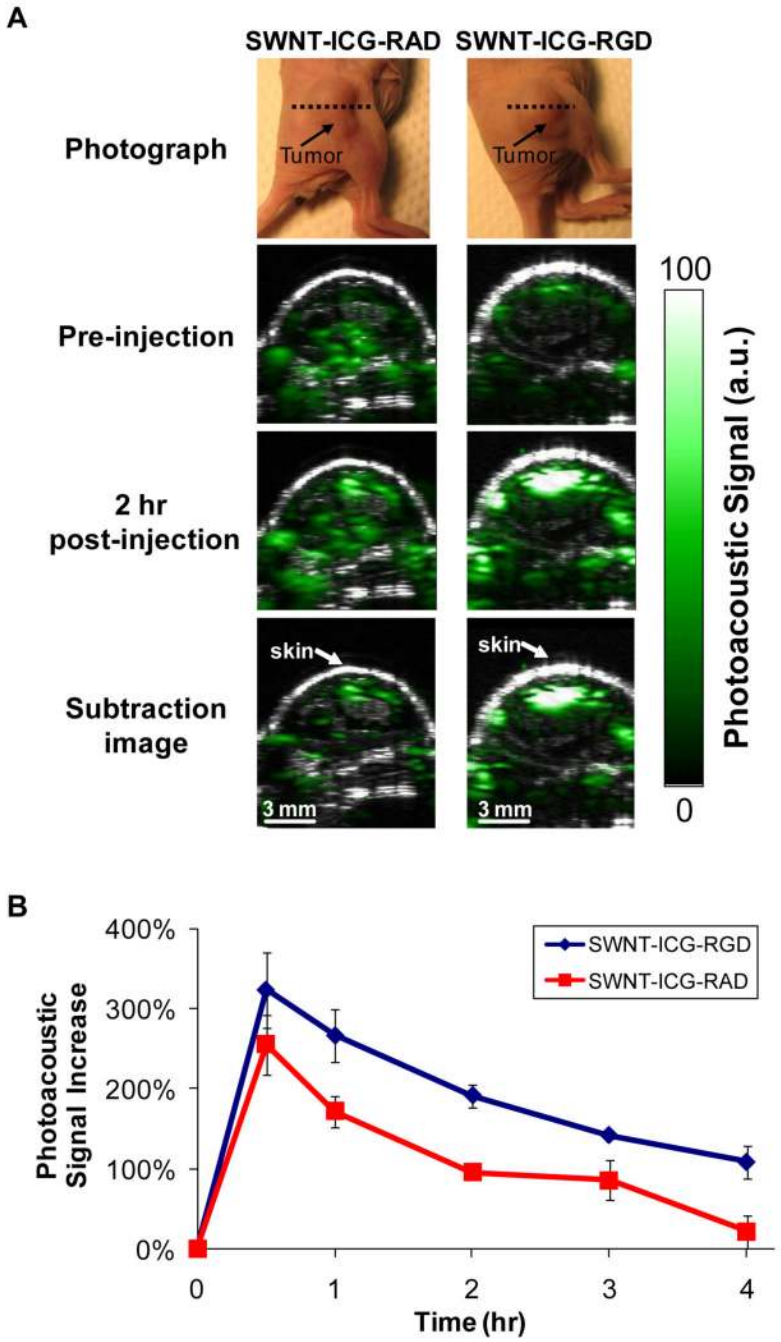

Figure 3. SWNT-ICG-RGD tumor targeting in living mice

(A) Ultrasound (gray) and photoacoustic (green) images of one vertical slice through the tumor (dotted black line). The ultrasound images show the skin and the tumor boundaries. Subtraction photoacoustic images were calculated as 2 hr post-injection minus pre-injection images. As can be seen in the subtraction images, SWNT-ICG-RGD accumulates in higher amount in the tumor as compared to the control SWNT-ICG-RAD. **(B)** Mice injected with SWNT-ICG-RGD showed significantly higher photoacoustic signal than mice injected with the untargeted control SWNT-ICG-RAD ($p < 0.001$). The error bars represent standard error ($n = 4$ mice)

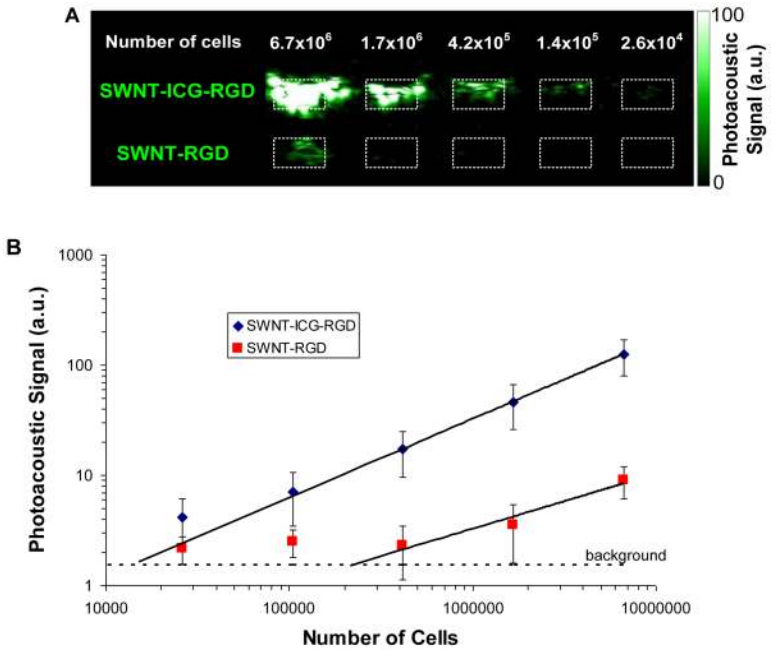

Figure 4. Comparison of plain SWNT-RGD to SWNT-ICG-RGD

(A) Photoacoustic vertical slice image through an agarose phantom containing increasing number of U87 cancer cells exposed to SWNT-ICG-RGD and plain SWNT-RGD particles. While 1.7×10^6 cells exposed to SWNT-RGD are barely seen on the image, a clear photoacoustic signal was observed from 1.4×10^5 cells exposed to SWNT-ICG-RGD. The signal inside the ROI (dotted white boxes) is not homogenous due to possible aggregates of cells. **(B)** Quantitative analysis of the photoacoustic signals from the phantom (n = 3) showed that SWNT-ICG-RGD can visualize ~20-times less cancer cells than SWNT-RGD can ($p < 0.0001$). The background line represents the average background signal in the phantom. Linear regression was calculated on the linear regime of both curves.